KYBERNETIKA — VOLUME *55* (2019), NUMBER 2, PAGES 385–401

A PRACTICAL SOLUTION TO IMPLEMENT NONLINEAR OUTPUT REGULATION VIA DYNAMIC MAPPINGS

Carlos Armenta, Jorge Álvarez, Raymundo Márquez, and Miguel Bernal

This paper presents a novel error-feedback practical solution for real-time implementation of nonlinear output regulation. Sufficient and necessary conditions for both state- and error-feedback output regulation have been established for linear and nonlinear systems several decades ago. In their most general form, these solutions require solving a set of nonlinear partial differential equations, which may be hard or even impossible to solve analytically. In recent years, a methodology for dynamic calculation of the mappings required for state-feedback regulation has been put forward; following the latter, an error-feedback extension is hereby provided which, when combined with design conditions in the form of linear matrix inequalities, becomes suitable for real-time setups. Real-time results are presented for a nonlinear twin rotor MIMO system. Issues concerning the implementation as well as the solutions adopted, are discussed.

Keywords: nonlinear output regulation, linear matrix inequality, twin rotor, real-time

Classification: 93C10, 93C95, 93D05

1. INTRODUCTION

This paper is concerned with nonlinear output regulation and its real-time implementation issues; a proposal based on the dynamic computing of the required steady-state maps and the use of convex optimization for determining the required gains is proven to systematically tackle them.

Output regulation consists in finding a control law able to asymptotically drive to zero an error signal which depends on the system outputs and the (quasi) periodic trajectories of an exosystem [15]; trajectory tracking of time-varying trajectories is therefore a particular case of it [18, 20]. Thus, output regulation generalizes the class of error signals to possibly nonlinear functions of the plant states and the exosystem with a variety of applications [14, 17, 35]. A typical regulation control law has two parts: one that drives the system to the desired manifold (reaching phase); another one that keeps it in the steady-state regime (steady-state phase).

Linear output regulation, also known as the servomechanism problem [8, 34], has been studied since the seminal work of [12]. Sufficient and necessary conditions where the control law depends on fully-available states or only on the error are given in [11]: they are based on solving algebraic linear equations. The solutions in these works were

DOI: 10.14736/kyb-2019-2-0385

reformulated in terms of linear matrix inequalities (LMIs) in [2], which can be efficiently solved via convex optimization techniques [4]. Since linear output regulation is easy to implement, most of real-time applications consider a linearized form of the model [13, 19].

Sufficient and necessary conditions for both state- and error-feedback *nonlinear output regulation*, first appeared in [16]: these results were derived using very involved developments from the field of geometric control, which in turn is based on differential geometry [15]. Error-feedback configurations are also based on the internal model principle [5]; along this path several results have appeared enhancing non-equilibrium theory [6], guaranteeing uniform practical regulation [22], and handling uncertain systems [7]; these approaches are intentionally left out of this paper.

Problem statement: Solving a nonlinear output regulation problem requires dealing with nonlinear partial differential equations, whose analytical solution –if available– might be impossible to obtain [21]; this has precluded real-time applications of this theory [27, 33]. Several works aimed to tackle this problem via Takagi-Sugeno models, but the solutions thus found remained approximate [23, 3]; some others converted some of the partial differential equations into ordinary ones, thus easing the former requirement of finding explicit analytical solutions [24, 29]. The latter has been referred to as *dynamic mappings*; it is only available for state feedback, which hinders its application to real-time setups where very often the full state is not available.

Contribution: A practical solution to perform nonlinear output regulation in the error-feedback case by determining: (a) controller and observer gains of the reaching phase via LMIs that meet real-time performance specifications, (b) dynamic mappings for the steady-state phase that avoid explicit solving of partial differential equations. Real-time implementation results of the proposed approach are provided for a nonlinear twin rotor MIMO system whose states are not fully available.

Organization: The theoretical proposal is presented in two parts: section 2 formulates an LMI approach for determining the controller gains involved in the reaching phase; section 3 develops a methodology for the dynamic calculation of the mappings required during the steady-state phase of the nonlinear error-feedback case. The practical contribution via real-time implementation is also twofold: the LMI solution for the reaching phase along with the dynamic mappings for the steady-state stage in order to perform regulation in a highly nonlinear MIMO twin rotor system [10, 26] in section 4. Issues concerning implementation as well as the solutions adopted, are discussed. Conclusions are drawn in section 5.

2. AN LMI SOLUTION FOR THE REACHING PHASE

In this section we are concerned with the reaching phase which drives the system states towards the desired manifold; its solution is the same for both the linear and nonlinear case via linearization[1].

[1]Indeed, as shown in Chapter 8 of [15], controller/observer design of the reaching phase for the nonlinear case can be achieved via linearization.

2.1. Preliminaries

Consider the following linear setup:

$$\dot{\mathbf{x}}(t) = \mathbf{A}\mathbf{x}(t) + \mathbf{B}\mathbf{u}(t), \tag{1}$$

$$\dot{\mathbf{w}}(t) = \mathbf{S}\mathbf{w}(t), \tag{2}$$

$$\mathbf{e}(t) = \mathbf{C}\mathbf{x}(t) + \mathbf{Q}\mathbf{w}(t), \tag{3}$$

where $\mathbf{x}(t) \in X \subset \mathbb{R}^n$ is the state vector of a plant, $\mathbf{w}(t) \in W \subset \mathbb{R}^q$ is the state vector of an exosystem which generates periodic signals[2], $\mathbf{e}(t) \in \mathbb{R}^m$ is a linear function of $\mathbf{x}(t)$ and $\mathbf{w}(t)$ known as the error signal, $\mathbf{u}(t) \in \mathbb{R}^m$ is the control input; $\mathbf{A}$, $\mathbf{B}$, $\mathbf{C}$, $\mathbf{Q}$, and $\mathbf{S}$ are known matrices of proper dimensions. It is assumed that $(\mathbf{x}, \mathbf{w}) = (\mathbf{0}, \mathbf{0})$ is an equilibrium point of the system with $\mathbf{u}(t) = \mathbf{0}$.

The *linear state-feedback output regulation problem* (LSFORP) consists in finding

$$\mathbf{u}(t) = \mathbf{K}\mathbf{x}(t) + \mathbf{L}\mathbf{w}(t) \quad \text{such that} \quad \lim_{t\to\infty} \mathbf{e}(t) = \mathbf{0} \tag{4}$$

for any initial condition $(\mathbf{x}(0), \mathbf{w}(0)) \in \Omega \subset X \times W$ with $(\mathbf{A} + \mathbf{B}\mathbf{K})$ Hurwitz (such that the system is stabilized by $\mathbf{u}(t)$ when $\mathbf{w}(t) = \mathbf{0}$).

The LSFORP has a solution if and only if [11]:

1. $\mathrm{Re}\{\sigma(\mathbf{S})\} \geq 0$ and $(\mathbf{A}, \mathbf{B})$ is stabilizable,
2. $\exists \mathbf{\Pi} \in \mathbb{R}^{n\times q}$, $\exists \mathbf{\Gamma} \in \mathbb{R}^{m\times q}$ such that

$$\mathbf{\Pi}\mathbf{S} = \mathbf{A}\mathbf{\Pi} + \mathbf{B}\mathbf{\Gamma}, \quad \mathbf{0} = \mathbf{C}\mathbf{\Pi} + \mathbf{Q}. \tag{5}$$

The gains in the control law (4) are thus $\mathbf{K}$ such that $(\mathbf{A} + \mathbf{B}\mathbf{K})$ is Hurwitz and $\mathbf{L} = \mathbf{\Gamma} - \mathbf{K}\mathbf{\Pi}$.

The LSFORP requires all the states to be available, which in real-time applications is hardly the case; thus, an observer must be somehow incorporated in the controller design to reconstruct the states through the only signal truly available: the error $\mathbf{e}(t)$.

The *linear error-feedback output regulation problem* (LEFORP) consists in finding an error-fed dynamic observer-based control law of the form

$$\dot{\boldsymbol{\xi}}(t) = \mathbf{F}\boldsymbol{\xi}(t) + \mathbf{G}\mathbf{e}(t), \quad \mathbf{u}(t) = \mathbf{H}\boldsymbol{\xi}(t), \tag{6}$$

where $\boldsymbol{\xi}(t) = \begin{bmatrix}\boldsymbol{\xi}_f^T(t) & \boldsymbol{\xi}_s^T(t)\end{bmatrix}^T \in \Xi \subset \mathbb{R}^{n+q}$, $\boldsymbol{\xi}_f(t) \in \mathbb{R}^n$ goes to $\mathbf{x}(t)$ as $t \to \infty$, $\boldsymbol{\xi}_s(t) \in \mathbb{R}^q$ goes to $\mathbf{w}(t)$ as $t \to \infty$, while $\mathbf{F} \in \mathbb{R}^{(n+q)\times(n+q)}$, $\mathbf{G} = \begin{bmatrix}\mathbf{G}_0^T & \mathbf{G}_1^T\end{bmatrix}^T$, $\mathbf{G}_0 \in \mathbb{R}^{n\times m}$, $\mathbf{G}_1 \in \mathbb{R}^{q\times m}$, and $\mathbf{H} \in \mathbb{R}^{m\times(n+q)}$ are designed to guarantee that $\forall(\mathbf{x}(0), \boldsymbol{\xi}(0), \mathbf{w}(0)) \in \Omega \subset X \times \Xi \times W$, the error (3) goes to zero and $\begin{bmatrix}\mathbf{A} & \mathbf{B}\mathbf{H} \\ \mathbf{G}\mathbf{C} & \mathbf{F}\end{bmatrix}$ is Hurwitz, so the control $\mathbf{u}(t)$ stabilizes the system when $\mathbf{w}(t) = \mathbf{0}$.

The LEFORP has a solution if and only if [11]:

[2]By definition, as shown in [11], a linear exosystem (2) is such that $\mathrm{Re}(\sigma(\mathbf{S})) = 0$, where $\sigma(\mathbf{S})$ stands for the spectrum of S.

1. $\mathrm{Re}\{\sigma(\mathbf{S})\} \geq 0$, $(\mathbf{A}, \mathbf{B})$ is stabilizable, and the pair $\left(\begin{bmatrix}\mathbf{A} & \mathbf{0}\\ \mathbf{0} & \mathbf{S}\end{bmatrix}, [\mathbf{C} \quad \mathbf{Q}]\right)$ is detectable.
2. $\exists \mathbf{\Pi} \in \mathbb{R}^{n\times q}$, $\exists \mathbf{\Gamma} \in \mathbb{R}^{m\times q}$ such that (5) holds.

Thus, the gains involved in the dynamic control law (6) are $\mathbf{K}$ such that $(\mathbf{A}+\mathbf{BK})$ is Hurwitz, $\mathbf{G}$ such that the observable modes of $\left(\begin{bmatrix}\mathbf{A} & \mathbf{0}\\ \mathbf{0} & \mathbf{S}\end{bmatrix} - \begin{bmatrix}\mathbf{G}_0\\ \mathbf{G}_1\end{bmatrix}[\mathbf{C} \quad \mathbf{Q}]\right)$ are stable, $\mathbf{F} = \begin{bmatrix}\mathbf{A}-\mathbf{G}_0\mathbf{C}+\mathbf{BK} & -\mathbf{G}_0\mathbf{Q}+\mathbf{B}(\mathbf{\Gamma}-\mathbf{K\Pi})\\ -\mathbf{G}_1\mathbf{C} & \mathbf{S}-\mathbf{G}_1\mathbf{Q}\end{bmatrix}$, and $\mathbf{H} = [\mathbf{K} \quad \mathbf{\Gamma}-\mathbf{K\Pi}]$.

2.2. An LMI proposal

The solutions in the preceding section are not optimal nor application-oriented; this is to say that for a concrete plant they cannot guarantee any physically viable controller/observer for the reaching phase. This might translate into low-energy responses that fall short from the control objective or saturation of the actuators. The LMI framework, on the other hand, provides a strategy for systematically incorporating such constraints [4].

In [2], element-wise LMIs were first employed to obtain the gains and mappings described above in a single step via convex optimization techniques; based on it, we propose the next application-oriented LMI result to calculate the gains $\mathbf{K}$ and $\mathbf{G}$ that solve the reaching phase of a LEFORP with a given decay rate[3] that ensures the observer converges at a given rate α_o faster than the controller rate α_c while avoiding input saturation by imposing $\|\mathbf{u}(t)\| \leq \mu$.

Theorem 2.1. During the reaching phase, the LEFORP has a solution with controller and observer decay rate of α_c and α_o, respectively, $0 < \alpha_c < \alpha_o$, and input constraint $\|\mathbf{u}(t)\| \leq \mu$ from a given initial condition $\mathbf{x}_0$, if there exists matrices $\mathbf{X} > 0$, $\mathbf{Y} > 0$, $\mathbf{M}$, and $\mathbf{N}$, such that the following LMIs hold:

$$He\left(\mathbf{AX}+\mathbf{BM}\right) + 2\alpha_c\mathbf{X} < 0, \tag{7}$$

$$He\left(\mathbf{Y}\begin{bmatrix}\mathbf{A} & \mathbf{0}\\ \mathbf{0} & \mathbf{S}\end{bmatrix} - \mathbf{N}\begin{bmatrix}\mathbf{C} & \mathbf{Q}\end{bmatrix}\right) + 2\alpha_o\mathbf{Y} < 0, \tag{8}$$

$$\begin{bmatrix}\mathbf{X} & \mathbf{M}^T\\ \mathbf{M} & \mu^2\mathbf{I}\end{bmatrix} \geq 0, \begin{bmatrix}1 & \mathbf{x}^T(0)\\ \mathbf{x}(0) & \mathbf{X}\end{bmatrix} \geq 0, \tag{9}$$

where $He(\cdot)$ is an operator defined as $He(\mathbf{D}) = \mathbf{D}+\mathbf{D}^T$. The controller gain is given by $\mathbf{K} = \mathbf{M}\mathbf{X}^{-1}$, the observer gains by $\mathbf{G} = \mathbf{Y}^{-1}\mathbf{N}$. Alternatively, controller and observer gains can be determined via pole placement by replacing (7) and (8) with the following LMIs:

$$\min \epsilon > 0 :$$

$$-\epsilon \prec He(\mathbf{AX}+\mathbf{BM}) - \mathbf{XJ}_1 \prec \epsilon \tag{10}$$

$$-\epsilon \prec He\left(\mathbf{Y}\begin{bmatrix}\mathbf{A} & \mathbf{0}\\ \mathbf{0} & \mathbf{S}\end{bmatrix} - \mathbf{N}\begin{bmatrix}\mathbf{C} & \mathbf{Q}\end{bmatrix}\right) - \mathbf{YJ}_2 \prec \epsilon \tag{11}$$

[3]The closed-loop linear system $\dot{\mathbf{x}}(t) = (\mathbf{A}+\mathbf{BK})\mathbf{x}(t)$ has a *decay rate* $\alpha > 0$ if and only if $\dot{V}(\mathbf{x}) \leq -2\alpha V(\mathbf{x})$, where $V(\mathbf{x})$ is an associated Lyapunov function.

where $\mathbf{J}_1$ and $\mathbf{J}_2$ are diagonal matrices whose entries correspond to the desired eigenvalues as long as their maxima are $-\alpha_c$ and $-\alpha_o$, respectively; $\prec$ stands for element-wise negative order relations.

P r o o f . Recall that the separation principle holds for linear systems; this is to say that the controller and the observer can be designed independently. Since decay rate α_c means that $\dot{V} \leq -2\alpha_c V$ for an associated Lyapunov function, consider $V(\mathbf{x}) = \mathbf{x}^T\mathbf{X}^{-1}\mathbf{x}$ with $\mathbf{X} > 0$ as a Lyapunov function candidate. The decay rate condition directly translates into (7) for the closed-loop system matrix $\mathbf{A}+\mathbf{BK}$; the same goes for the alternative LMI (10) since the element-wise form ensures the matrix $\mathbf{A}+\mathbf{BK}$ has the same eigenvalues of $\mathbf{J}_1$ [32], the fact that $-\alpha_c$ is the maximum eigenvalue ensures decay rate of α_c [9].

Similarly, $\left(\begin{bmatrix}\mathbf{A} & \mathbf{0}\\ \mathbf{0} & \mathbf{S}\end{bmatrix} - \begin{bmatrix}\mathbf{G}_0\\ \mathbf{G}_1\end{bmatrix}[\mathbf{C} \quad \mathbf{Q}]\right)$ is the closed-loop system matrix for the observer because it observes the system and the exosystem states $\mathbf{x}$ and $\mathbf{w}$. Considering a Lyapunov function candidate $V(\mathbf{e}_o) = \mathbf{e}_o^T\mathbf{Y}\mathbf{e}_o$ with $\mathbf{Y} > 0$ and the observation error $\mathbf{e}_o = \left[\mathbf{x}^T - \boldsymbol{\zeta}_f^T \quad \mathbf{w}^T - \boldsymbol{\zeta}_s^T\right]^T$, the same reasoning as before leads to LMIs (8) (or, alternatively, to (11)).

Holding an input constraint $\mu > 0$ for a given initial condition $\mathbf{x}_0$ is equivalent to $\|u\|^2 = u^T u \leq \mu^2$. which, along with restrictions on the Lyapunov function such that $V \leq V(0) \leq 1$, can be translated into a standard LMI (9) as shown in [9]; this concludes the proof. □

The previous theorem is concerned with the reaching phase, but mappings $\boldsymbol{\Pi}$ and $\boldsymbol{\Gamma}$, which are involved in the steady-state phase, can also be found simultaneously via element-wise LMIs that implement (5) (see [2] for details).

3. NONLINEAR REGULATION

In this section we are concerned with the steady-state phase of nonlinear output regulation. Once the preliminaries are presented, a second application-oriented contribution for implementing the required nonlinear mappings in real-time setups whose state might not be fully available is presented.

3.1. Preliminaries

Consider the following nonlinear system setup:

$$\dot{\mathbf{x}}(t) = \mathbf{f}(\mathbf{x}(t)) + \mathbf{g}(\mathbf{x}(t))\mathbf{u}(t) \tag{12}$$

$$\dot{\mathbf{w}}(t) = \mathbf{s}(\mathbf{w}(t)) \tag{13}$$

$$\mathbf{e}(t) = \mathbf{h}(\mathbf{x}(t)) + \mathbf{q}(\mathbf{w}(t)), \tag{14}$$

where $\mathbf{x}(t)$, $\mathbf{u}(t)$, $\mathbf{w}(t)$, and $\mathbf{e}(t)$ are the system state, the control input, the exosystem state (quasi-periodic or periodic), and the error function, respectively, while $\mathbf{f}(\mathbf{x}(t))$, $\mathbf{g}(\mathbf{x}(t))$, $\mathbf{s}(\mathbf{w}(t))$, $\mathbf{h}(\mathbf{x}(t))$, and $\mathbf{q}(\mathbf{w}(t))$ are (possibly nonlinear) vector functions of adequate size.

Nonlinear state-feedback output regulation problem (NLSFORP): Consists in finding

$$\mathbf{u}(t) = \boldsymbol{\alpha}(\mathbf{x}(t), \mathbf{w}(t)) \quad \text{such that} \quad \lim_{t\to\infty} \mathbf{e}(t) = \mathbf{0} \tag{15}$$

for any initial condition $(\mathbf{x}(0), \mathbf{w}(0)) \in \Omega \subset X \times W$ (in a neighbourhood of $(\mathbf{0}, \mathbf{0})$) as well as guaranteeing $\mathbf{x}{=}\mathbf{0}$ is an exponentially stable equilibrium point of (12) with $\mathbf{w}(t){=}\mathbf{0}$.

The NLSFORP has a solution if and only if [16]:

1. $\mathbf{w}(t){=}\mathbf{0}$ is an equilibrium point with a neighborhood $\tilde{W} \subset W$ in which every initial condition $\mathbf{w}(0)$ is Poisson stable[4], and the pair $(\mathbf{f}(\mathbf{x}), \mathbf{g}(\mathbf{x}))$ has a stabilizable linear approximation $(\mathbf{A}, \mathbf{B})$ at $\mathbf{x}{=}\mathbf{0}$.

2. $\exists \mathbf{x}{=}\boldsymbol{\pi}(\mathbf{w})$ with $\boldsymbol{\pi}(\mathbf{0}){=}\mathbf{0}$ and $\exists \mathbf{u}{=}\boldsymbol{\gamma}(\mathbf{w})$ with $\boldsymbol{\gamma}(\mathbf{0}){=}\mathbf{0}$, both mappings $\mathscr{C}^k$ $(k \geq 2)$ defined in a neighborhood $W^o \subset W$ of $\mathbf{w}(t){=}\mathbf{0}$, satisfying the *Francis-Isidori-Byrnes* (FIB) conditions

$$\frac{\partial \boldsymbol{\pi}}{\partial \mathbf{w}} \mathbf{s}(\mathbf{w}) = \mathbf{f}\left(\boldsymbol{\pi}(\mathbf{w})\right) + \mathbf{g}\left(\boldsymbol{\pi}(\mathbf{w})\right) \boldsymbol{\gamma}(\mathbf{w}), \tag{16}$$

$$\mathbf{0} = \mathbf{h}\left(\boldsymbol{\pi}(\mathbf{w})\right) + \mathbf{q}(\mathbf{w}). \tag{17}$$

Thus, the control law performing the regulation task for every initial condition in W^o is

$$\mathbf{u}(t) = \boldsymbol{\alpha}(\mathbf{x}(t), \mathbf{w}(t)) = \boldsymbol{\gamma}(\mathbf{w}(t)) + \mathbf{K}\left(\mathbf{x}(t) - \boldsymbol{\pi}(\mathbf{w}(t))\right), \tag{18}$$

where $\mathbf{K}$ is any gain such that $(\mathbf{A} + \mathbf{B}\mathbf{K})$ is Hurwitz for $\mathbf{A} = \partial \mathbf{f}/\partial \mathbf{x}|_{\mathbf{x}=\mathbf{0}}$, $\mathbf{B} = \mathbf{g}(\mathbf{0})$.

As mentioned earlier, the state may not be available to perform output regulation. An usual answer to this problem consists in designing an observer which reconstructs the state based on the output (the error signal $\mathbf{e}(t)$ in this case). This is the purpose behind the construction of a dynamical controller whose internal model is supposed to eventually match both the system and the exosystem. To this end, consider the following dynamical controller:

$$\dot{\boldsymbol{\xi}}(t) = \boldsymbol{\eta}\left(\boldsymbol{\xi}, \mathbf{e}\right), \quad \mathbf{u} = \boldsymbol{\theta}\left(\boldsymbol{\xi}\right) \tag{19}$$

where $\boldsymbol{\xi} \in \Xi \subset \mathbb{R}^{n+q}$ is intended to observe both the system states $\mathbf{x}(t)$ and the exosystem ones $\mathbf{w}(t)$. It is assumed that $\boldsymbol{\eta}(\mathbf{0}, \mathbf{0}) = \mathbf{0}$ and $\boldsymbol{\theta}(\mathbf{0}) = \mathbf{0}$, so the closed-loop system

$$\begin{aligned} \dot{\mathbf{x}}(t) &= \mathbf{f}(\mathbf{x}) + \mathbf{g}(\mathbf{x})\boldsymbol{\theta}(\boldsymbol{\xi}) \\ \dot{\boldsymbol{\xi}}(t) &= \boldsymbol{\eta}\left(\boldsymbol{\xi}, \mathbf{h}(\mathbf{x}) + \mathbf{q}(\mathbf{w})\right) \\ \dot{\mathbf{w}}(t) &= \mathbf{s}(\mathbf{w}) \end{aligned} \tag{20}$$

has an equilibrium at $(\mathbf{x}, \boldsymbol{\xi}, \mathbf{w}) = (\mathbf{0}, \mathbf{0}, \mathbf{0})$.

Nonlinear error-feedback output regulation problem (NLEFORP): Consists in finding an error-fed dynamic observer-based control law (19) such that $\forall\, (\mathbf{x}(0), \boldsymbol{\xi}(0), \mathbf{w}(0)) \in$

[4]A point $\mathbf{w}(0)$ is Poisson stable if the trajectory $\mathbf{w}(t)$ which contains it passes arbitrarily close to $\mathbf{w}(0)$ for arbitrarily large times, in forward and backward direction [15].

$\Omega \subset X \times \Xi \times W$ (in a neighbourhood of $(\mathbf{0}, \mathbf{0}, \mathbf{0})$), the closed-loop system (20) satisfies $\lim_{t\to\infty} \mathbf{e}(t) = \mathbf{0}$, and, if $\mathbf{w}(t) = \mathbf{0}$ then $\mathbf{q}(\mathbf{w}) = \mathbf{0}$, therefore the system

$$\begin{aligned} \dot{\mathbf{x}}(t) &= \mathbf{f}(\mathbf{x}) + \mathbf{g}(\mathbf{x})\boldsymbol{\theta}(\boldsymbol{\xi}) \\ \dot{\boldsymbol{\xi}}(t) &= \boldsymbol{\eta}\left(\boldsymbol{\xi}, \mathbf{h}(\mathbf{x})\right) \end{aligned} \tag{21}$$

has an equilibrium point at $(\mathbf{x}, \boldsymbol{\xi}) = (\mathbf{0}, \mathbf{0})$ which is exponentially stable.

The NLEFORP has a solution if and only if [16]:

1. $\mathbf{w}(t)$=$\mathbf{0}$ is an equilibrium point with a neighborhood $\tilde{W} \subset W$ in which every initial condition $\mathbf{w}(0)$ generates a Poisson stable trajectory,

2. provided $\mathbf{A}$, $\mathbf{B}$, and $\mathbf{C}$ are linear approximations of $\mathbf{f}(\mathbf{x})$, $\mathbf{g}(\mathbf{x})$, and $\mathbf{h}(\mathbf{x})$, respectively, the matrices $\mathbf{F} = (\partial\boldsymbol{\eta}/\partial\boldsymbol{\xi})|_{\boldsymbol{\xi}=\mathbf{0}}$ and $\mathbf{H} = (\partial\boldsymbol{\theta}/\partial\boldsymbol{\xi})|_{\boldsymbol{\xi}=\mathbf{0}}$ are such that the pair
$$\begin{pmatrix} \mathbf{A} & \mathbf{0} \\ \mathbf{GC} & \mathbf{F} \end{pmatrix}, \quad \begin{pmatrix} \mathbf{B} \\ \mathbf{0} \end{pmatrix} \tag{22}$$
is stabilizable for some choice of $\mathbf{G}$, and the pair
$$\begin{pmatrix} \mathbf{C} & \mathbf{0} \end{pmatrix}, \quad \begin{pmatrix} \mathbf{A} & \mathbf{BH} \\ \mathbf{0} & \mathbf{F} \end{pmatrix} \tag{23}$$
is detectable.

3. $\exists \mathbf{x} = \boldsymbol{\pi}(\mathbf{w})$ with $\boldsymbol{\pi}(\mathbf{0}) = \mathbf{0}$ and $\exists \mathbf{u} = \boldsymbol{\gamma}(\mathbf{w})$ with $\boldsymbol{\gamma}(\mathbf{0}) = \mathbf{0}$ such that (16)-(17) hold for any $\mathbf{w}(t) \in W^0 \subset W \supset \mathbf{0}$.

4. the exosystem with output $\{W^o, \mathbf{s}, \boldsymbol{\gamma}\}$ is immersed into the system (19) with $\mathbf{e}(t) = \mathbf{0}$, i. e., into $\dot{\boldsymbol{\xi}} = \boldsymbol{\eta}\left(\boldsymbol{\xi}, \mathbf{0}\right)$, $\mathbf{u} = \boldsymbol{\theta}\left(\boldsymbol{\xi}\right)$, defined on a neighborhood Ξ^o of the origin in $\mathbb{R}^{n+q}$ in which $\boldsymbol{\eta}(\mathbf{0}) = \mathbf{0}$ and $\boldsymbol{\theta}(\mathbf{0}) = \mathbf{0}$.

Splitting $\boldsymbol{\xi}$ as $\boldsymbol{\xi} = \begin{bmatrix} \boldsymbol{\xi}_f^T & \boldsymbol{\xi}_s^T \end{bmatrix}^T$, with $\boldsymbol{\xi}_f \in \mathbb{R}^n$, $\boldsymbol{\xi}_s \in \mathbb{R}^q$, the control law in (19) achieving error-feedback output regulation for every initial condition in W^o is

$$\mathbf{u}\left(\boldsymbol{\xi}_f, \boldsymbol{\xi}_s\right) = \boldsymbol{\theta}(\boldsymbol{\xi}) = \boldsymbol{\gamma}\left(\boldsymbol{\xi}_s\right) + \mathbf{K}\left(\boldsymbol{\xi}_f - \boldsymbol{\pi}\left(\xi_s\right)\right), \tag{24}$$

where $\boldsymbol{\xi}_f$ and $\boldsymbol{\xi}_s$ are dynamically implemented by splitting $\boldsymbol{\eta}(\cdot,\cdot) = \begin{bmatrix} \boldsymbol{\eta}_f^T(\cdot,\cdot) & \boldsymbol{\eta}_s^T(\cdot,\cdot) \end{bmatrix}^T$ in order to fit

$$\begin{aligned} \dot{\boldsymbol{\xi}}_f = \boldsymbol{\eta}_f\left(\boldsymbol{\xi}_f, \boldsymbol{\xi}_s, \mathbf{e}\right) &= \mathbf{f}\left(\boldsymbol{\xi}_f\right) + \mathbf{g}\left(\boldsymbol{\xi}_f\right)\mathbf{u}\left(\boldsymbol{\xi}_f, \boldsymbol{\xi}_s\right) \\ &\quad - \mathbf{G}_1\big(\mathbf{h}\left(\boldsymbol{\xi}_f\right) + \mathbf{q}\left(\boldsymbol{\xi}_s\right) - \mathbf{e}\big) \\ \dot{\boldsymbol{\xi}}_s = \boldsymbol{\eta}_s\left(\boldsymbol{\xi}_f, \boldsymbol{\xi}_s, \mathbf{e}\right) &= \mathbf{s}\left(\boldsymbol{\xi}_s\right) - \mathbf{G}_2\big(\mathbf{h}\left(\boldsymbol{\xi}_f\right) + \mathbf{q}\left(\boldsymbol{\xi}_s\right) - \mathbf{e}\big), \end{aligned} \tag{25}$$

where $\mathbf{G} = \begin{bmatrix} \mathbf{G}_1^T & \mathbf{G}_2^T \end{bmatrix}^T$.

3.2. A dynamic mapping proposal

Solving nonlinear partial differential equations such as (16) – (17) to find the steady-state nonlinear mappings $\boldsymbol{\pi}(\mathbf{w})$ and $\boldsymbol{\gamma}(\mathbf{w})$ is a difficult task, especially for high-order systems; moreover, even if these mappings are found, they might be too involved for real-time implementation. The methodology in [24], corrected in [29], tackles this problem by relaxing the requirement of finding an *explicit static mapping* $\boldsymbol{\pi}(\mathbf{w})$; instead, *implicit dynamic mappings* are used. This novel methodology – depicted in Figure 1 – is hereby extended to the error-feedback case.

To do so, consider the class of nonlinear systems whose equations (12) – (14) can be rewritten as follows:

$$\dot{\mathbf{x}}(t) = \mathbf{A}(\mathbf{x}(t))\mathbf{x}(t) + \mathbf{B}(\mathbf{x}(t))\mathbf{u}(t), \tag{26}$$

$$\dot{\mathbf{w}}(t) = \mathbf{S}(\mathbf{w}(t))\mathbf{w}(t), \tag{27}$$

$$\mathbf{e}(t) = \mathbf{C}(\mathbf{x}(t))\mathbf{x}(t) + \mathbf{Q}(\mathbf{w}(t))\mathbf{w}(t), \tag{28}$$

where (possibly nonlinear) matrix expressions $\mathbf{A}(\mathbf{x})$, $\mathbf{B}(\mathbf{x})$, $\mathbf{S}(\mathbf{w})$, $\mathbf{C}(\mathbf{x})$, and $\mathbf{Q}(\mathbf{w})$ are well defined with $\sigma(\mathbf{S}(\mathbf{0})) \subset \mathbb{I}$.

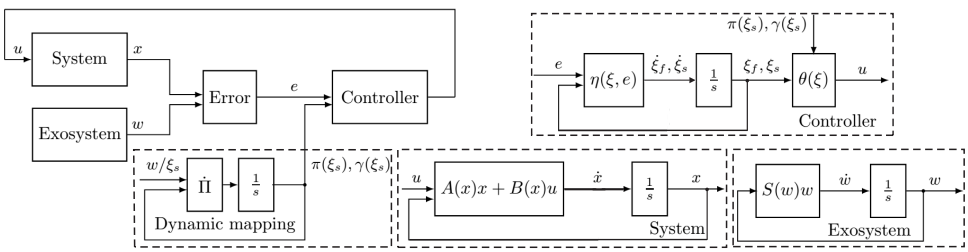

Fig. 1: Block diagram for Dynamic Nonlinear Error-Feedback Output Regulation.

Theorem 3.1. Given a nonlinear setup as described in (26) – (28) along with a dynamical controller of the form (19) with closed-loop structure (25), the NLEFORP has a solution if: (a) there exists matrices $\mathbf{X} > 0$, $\mathbf{Y} > 0$, $\mathbf{M}$, and $\mathbf{N}$, such that LMIs (7) – (9) hold for given constants $\alpha_c, \alpha_o, \mu > 0$, initial condition $\mathbf{x}_0$, and matrices $\mathbf{A} = \mathbf{A}(\mathbf{0})$, $\mathbf{B} = \mathbf{B}(\mathbf{0})$, $\mathbf{S} = \mathbf{S}(\mathbf{0})$, $\mathbf{C} = \mathbf{C}(\mathbf{0})$, and $\mathbf{Q} = \mathbf{Q}(\mathbf{0})$; (b) there exist possibly nonlinear matrix functions $\boldsymbol{\Pi}(\mathbf{w})$ and $\boldsymbol{\Gamma}(\mathbf{w})$ such that

$$\dot{\boldsymbol{\Pi}}(\mathbf{w}) = \mathbf{A}(\boldsymbol{\Pi}(\mathbf{w})\mathbf{w})\boldsymbol{\Pi}(\mathbf{w}) + \mathbf{B}(\boldsymbol{\Pi}(\mathbf{w})\mathbf{w})\boldsymbol{\Gamma}(\mathbf{w}) - \boldsymbol{\Pi}(\mathbf{w})\mathbf{S}(\mathbf{w}), \tag{29}$$

$$\mathbf{0} = \mathbf{C}(\boldsymbol{\Pi}(\mathbf{w})\mathbf{w})\boldsymbol{\Pi}(\mathbf{w}) + \mathbf{Q}(\mathbf{w}). \tag{30}$$

The corresponding control law is given by

$$\mathbf{u}(t) = \boldsymbol{\Gamma}(\boldsymbol{\xi}_s)\boldsymbol{\xi}_s(t) + \mathbf{K}\left(\boldsymbol{\xi}_f - \boldsymbol{\Pi}(\boldsymbol{\xi}_f, \boldsymbol{\xi}_s)\boldsymbol{\xi}_s(t)\right). \tag{31}$$

Proof. Clearly, the matrices corresponding to linearization of (26) – (28) are $\mathbf{A} = \mathbf{A}(\mathbf{0})$, $\mathbf{B} = \mathbf{B}(\mathbf{0})$, $\mathbf{S} = \mathbf{S}(\mathbf{0})$, $\mathbf{C} = \mathbf{C}(\mathbf{0})$, and $\mathbf{Q} = \mathbf{Q}(\mathbf{0})$. Since $\sigma(\mathbf{S}(\mathbf{0})) \subset \mathbb{I}$, condition 1

for the NLEFORP to have a solution (see the previous section) is satisfied, i. e., trajectories are Poisson stable. Feasibility of LMIs (7) – (9) implies the existence of a local controller with gain $\mathbf{K}$ and a local observer with gain $\mathbf{G}$ whose linearization is the same as that of (25); thus, condition 2 for the solution of the NLEFORP is also satisfied by defining $\mathbf{F}$ and $\mathbf{H}$ in the same way as in section 2 (linear case).

Defining nonlinear mappings $\mathbf{x} = \boldsymbol{\pi}(\mathbf{w}) = \boldsymbol{\Pi}(\mathbf{w})\mathbf{w}$ and $\mathbf{u} = \boldsymbol{\gamma}(\mathbf{w}) = \boldsymbol{\Gamma}(\mathbf{w})\mathbf{w}$, condition 3 for solving the NLEFORP translates into rewriting (16) – (17) as:

$$\begin{aligned}\frac{\partial \boldsymbol{\pi}}{\partial \mathbf{w}}\mathbf{S}(\mathbf{w})\mathbf{w} = \dot{\boldsymbol{\pi}}(\mathbf{w}) = \dot{\boldsymbol{\Pi}}(\mathbf{w})\mathbf{w} + \boldsymbol{\Pi}(\mathbf{w})\dot{\mathbf{w}} = \dot{\boldsymbol{\Pi}}(\mathbf{w})\mathbf{w} + \boldsymbol{\Pi}(\mathbf{w})\mathbf{S}(\mathbf{w})\mathbf{w} \\ = \mathbf{A}(\boldsymbol{\Pi}(\mathbf{w})\mathbf{w})\boldsymbol{\Pi}(\mathbf{w})\mathbf{w} + \mathbf{B}(\boldsymbol{\Pi}(\mathbf{w})\mathbf{w})\boldsymbol{\Gamma}(\mathbf{w})\mathbf{w}, \\ \mathbf{0} = \mathbf{C}(\boldsymbol{\Pi}(\mathbf{w})\mathbf{w})\boldsymbol{\Pi}(\mathbf{w})\mathbf{w} + \mathbf{Q}(\mathbf{w})\mathbf{w},\end{aligned}$$

from which (29) – (30) can be straightforwardly obtained [24, 29].

Condition 4 for solvability of the NLEFORP is directly satisfied by construction of the dynamical controller (19) with closed-loop structure (25). Substituting the corresponding mappings in (24) we obtain (31), which concludes the proof. □

Scheme implementation: The proposed scheme requires solving equations (29) – (30) (a) for each entry of $\boldsymbol{\Gamma}$ and $\boldsymbol{\Pi}$ whenever an explicit solution is possible, or (b) for $\dot{\Pi}_{ij}$ at those entries (i, j) of $\boldsymbol{\Pi}$ where no explicit solution can be found: these are dynamically implemented, i. e., they are obtained on-line via integration of the differential equations that describe them [29].

Note that the entries of $\boldsymbol{\Pi}$ can be threefold: a constant $\Pi_{ij} = k$, an explicit static mapping $\Pi_{ij}(w)$ depending on $\mathbf{w}(t)$, or a dynamic mapping Π_{ij} which can be initialized at any value. This is not surprising as the FIB equations (16) – (17) are being satisfied by (not necessarily unique) mappings $\boldsymbol{\pi} = \boldsymbol{\Pi}\mathbf{w}$ and $\boldsymbol{\gamma} = \boldsymbol{\Gamma}\mathbf{w}$ (arguments omitted) satisfying (29) – (30).

Use of available signals in real-time setups: Notice that dynamic mappings for $\boldsymbol{\Pi}$ are fed with $\boldsymbol{\xi}_s(t)$, which is part of the observer state which follows $\mathbf{w}(t)$, the exosystem state. Nevertheless, real-time implementations can benefit from any knowledge of the plant and exosystem states, since usually some of the states of the former and all the states of the latter are known (the exosystem being normally an artificial setup for generating signals to be tracked).

Further improvements: Controller and observer design for the pairs

$$(\mathbf{A}(\mathbf{x}), \mathbf{B}(\mathbf{x})),\ \left(\left(\begin{bmatrix}\mathbf{A}(\mathbf{x}) & \mathbf{0} \\ \mathbf{0} & \mathbf{S}(\mathbf{w})\end{bmatrix}, \begin{bmatrix}\mathbf{C}(\mathbf{x}) & \mathbf{Q}(\mathbf{w})\end{bmatrix}\right)\right)$$

can be achieved through nonlinear techniques such as those based on exact convex models and LMIs [3, 30] instead of linear ones as before; this may increase the size of the neighbourhood on which regulation takes place, though at a higher computational price.

4. IMPLEMENTATION ON THE TWIN ROTOR

Modelling: The twin rotor intends to model in a simple way the dynamics of a helicopter; it is a MIMO system since there are two actuators (inputs) and two angles of

interest (outputs). Two DC motors are placed at the extreme points of a beam with a counterbalance pole at the middle, in order to control two helixes; these are oriented in azimuth and elevation angles. Besides the high-order and nonlinear characteristics of the plant, there is an important coupling between the two rotors. The plant by Feedback ^{TM} [10] is shown in Figure 2.

Several models of the twin rotor are available: 6-state simplified models that ignore the nonlinear coupling between the two rotors can be found in [25, 28, 31]; the states are the elevation x_2 and azimuth angles x_5, their corresponding angular velocities x_3 and x_6, and the motor speeds x_1 and x_4. On the other hand, the provider model is a 7-state one which incorporates an internal state x_7 which is a torque associated with the azimuth angle that relates both helixes [1, 10], a representation usually enlarged with two other states x_8 and x_9 which are the integrals of x_2 and x_5, respectively. Recall that only the angles x_2 and x_5 can be measured by the encoder sensors. Thus, the 9-state twin rotor model as expressed in (26), the exosystem generating sinusoidal references w_1 and w_2 to be followed by angles x_2 and x_5, and the corresponding error signal are the following:

$$\begin{bmatrix}\dot{x}_1\\ \dot{x}_2\\ \dot{x}_3\\ \dot{x}_4\\ \dot{x}_5\\ \dot{x}_6\\ \dot{x}_7\\ \dot{x}_8\\ \dot{x}_9\end{bmatrix} = \underbrace{\begin{bmatrix} 0.8333 & 0 & 0 & 0 & 0 & 0 & 0 & 0 & 0\\ 0 & 0 & 1 & 0 & 0 & 0 & 0 & 0 & 0\\ E_1 & E_2 & -\dfrac{B_{1\Psi}}{I_1} & 0 & 0 & E_3 & 0 & 0 & 0\\ 0 & 0 & 0 & -1 & 0 & 0 & 0 & 0 & 0\\ 0 & 0 & 0 & 0 & -1 & 0 & 0 & 0 & 0\\ 0 & 0 & 0 & E_4 & 0 & -\dfrac{B_{1\Phi}}{I_2} & -\dfrac{1}{I_2} & 0 & 0\\ E_5 & 0 & 0 & 0 & 0 & 0 & -\dfrac{1}{I_2} & 0 & 0\\ 0 & 1 & 0 & 0 & 0 & 0 & 0 & 0 & 0\\ 0 & 0 & 0 & 0 & 1 & 0 & 0 & 0 & 0\end{bmatrix}}_{\mathbf{A}(\mathbf{x}(t))} \begin{bmatrix}x_1\\ x_2\\ x_3\\ x_4\\ x_5\\ x_6\\ x_7\\ x_8\\ x_9\end{bmatrix} + \underbrace{\begin{bmatrix} 0.9166 & 0\\ 0 & 0\\ 0 & 0\\ 0 & 0.8\\ 0 & 0\\ 0 & 0\\ E_6 & 0\\ 0 & 0\\ 0 & 0\end{bmatrix}}_{\mathbf{B}(\mathbf{x}(t))} \begin{bmatrix}u_1\\ u_2\end{bmatrix},$$

$$\begin{bmatrix}\dot{w}_1\\ \dot{w}_2\end{bmatrix} = \underbrace{\begin{bmatrix}0 & 1\\ -1 & 0\end{bmatrix}}_{\mathbf{S}(\mathbf{w}(t))} \begin{bmatrix}w_1\\ w_2\end{bmatrix}, \quad \mathbf{e}(t) = \underbrace{\begin{bmatrix}0 & 1 & 0 & 0 & 0 & 0 & 0 & 0 & 0\\ 0 & 0 & 0 & 0 & 1 & 0 & 0 & 0 & 0\end{bmatrix}}_{\mathbf{C}(\mathbf{x})} \mathbf{x}(t) + \underbrace{\begin{bmatrix}-1 & 0\\ 0 & -1\end{bmatrix}}_{\mathbf{Q}(\mathbf{w})} \mathbf{w}(t),$$

$E_1 = (b_1 + a_1 x_1)(1 - K_{gy} x_6 \cos x_2)/I_1$, $E_2 = -M_g \sin x_2/(I_1 x_2)$, $E_3 = 0.0163 x_6 \sin(2x_2)/I_2$, $E_4 = (b_2 + a_2 x_4)/I_2$, $E_5 = 0.5 B_{cte}(b_1 + a_1 x_1) - A_{cte}(0.5 b_1 + a_1 x_1)$, $E_6 = 0.9166 A_{cte}(0.5 b_1 + a_1 x_1)$, and parameters taken from Table 1.

Dynamic mappings: Applying Theorem 3.1, equations (29) – (30) need to be solved according to the procedures described in section 3; to this end, every expression in them should be in terms of mapping entries Π_{ij} and Γ_{kj}, $i \in \{1, 2, \ldots, 9\}$, $j, k \in \{1, 2\}$, as well as w_1 and w_2, i. e., each x_i in $\mathbf{A}(\mathbf{x}(t))$, $\mathbf{B}(\mathbf{x}(t))$, and $\mathbf{C}(\mathbf{x}(t))$ should be replaced by

Fig. 2: The Twin Rotor MIMO System.

$x_i = \Pi_{i1} w_1 + \Pi_{i2} w_2$, $i \in \{1, 2, \ldots, 9\}$. From equation (30) yields:

$$\mathbf{0} = \underbrace{\begin{bmatrix} \Pi_{21} & \Pi_{22} \\ \Pi_{51} & \Pi_{52} \end{bmatrix}}_{\mathbf{C\Pi}} + \underbrace{\begin{bmatrix} -1 & 0 \\ 0 & -1 \end{bmatrix}}_{\mathbf{Q}} \quad \Rightarrow \quad \begin{array}{ll} \Pi_{21} = 1, & \Pi_{22} = 0, \\ \Pi_{51} = 0, & \Pi_{52} = 1. \end{array}$$

After substitution of these data in (29), the designer is faced with 18 equations corresponding to each $\dot{\Pi}_{ij}$. Most of these expressions are quite long, so only the variables they depend on are shown in Table 2; otherwise, they are explicitly stated. Notice that $\Pi_{31} = 0$, $\Pi_{32} = 1$, $\Pi_{61} = -1$, and $\Pi_{62} = 0$ follow directly from the fact that $\dot{\Pi}_{21} = \dot{\Pi}_{22} = \dot{\Pi}_{51} = \dot{\Pi}_{52} = 0$. Moreover, due to the simplicity of the equations in the last two rows of Table 2, which are isolated from the rest, the corresponding mappings can be straightforwardly given as $\Pi_{81} = 0$, $\Pi_{82} = -1$, $\Pi_{91} = 1$, and $\Pi_{92} = 0$.

Once the aforementioned constant terms are taken into account, it is found that the equations corresponding to $\dot{\Pi}_{31} = 0$ and $\dot{\Pi}_{32} = 0$ are only in terms of w_1, w_2, Π_{11},

Symbol	Description	Value	Units
I_1	Moment of inertia (vertical rotor)	0.068	kg·m^2
I_2	Moment of inertia (horizontal rotor)	0.02	kg·m^2
a_1	Static characteristic parameters	0.0135	-
b_1	Static characteristic parameters	0.0924	-
a_2	Static characteristic parameters	0.02	-
b_2	Static characteristic parameters	0.09	-
M_g	Gravity momentum	0.32	N·m
$B_{1\psi}$	Friction momentum parameter	0.006	N·m·s/rad
$B_{1\phi}$	Friction momentum parameter	0.1	N·m·s/rad
K_{gy}	Gyroscopic momentum parameter	0.05	s/rad
A_{cte}	Constant related to coupling state	-0.7	-
B_{cte}	Constant related to coupling state	-0.2	-

Tab. 1: Twin Rotor parameters.

$\dot{\Pi}_{ij}$ depends on	
$\dot{\Pi}_{11}:\ \Gamma_{11}, \Pi_{11}, \Pi_{12}$	$\dot{\Pi}_{12}:\ \Gamma_{12}, \Pi_{11}, \Pi_{12}$
$\dot{\Pi}_{21} = \Pi_{31} = 0$	$\dot{\Pi}_{22} = \Pi_{32} - 1 = 0$
$\dot{\Pi}_{31}:\ w_1, w_2, \Pi_{11}, \Pi_{12}, \Pi_{31}, \Pi_{32}, \Pi_{61}, \Pi_{62}$	$\dot{\Pi}_{32}:\ w_1, w_2, \Pi_{11}, \Pi_{12}, \Pi_{31}, \Pi_{32}, \Pi_{61}, \Pi_{62}$
$\dot{\Pi}_{41}:\ \Gamma_{21}, \Pi_{41}, \Pi_{42}$	$\dot{\Pi}_{42}:\ \Gamma_{22}, \Pi_{41}, \Pi_{42}$
$\dot{\Pi}_{51} = \Pi_{61} + 1 = 0$	$\dot{\Pi}_{52} = \Pi_{62} = 0$
$\dot{\Pi}_{61}:\ w_1, w_2, \Pi_{41}, \Pi_{42}, \Pi_{61}, \Pi_{62}, \Pi_{71}$	$\dot{\Pi}_{62}:\ w_1, w_2, \Pi_{41}, \Pi_{42}, \Pi_{61}, \Pi_{62}, \Pi_{72}$
$\dot{\Pi}_{71}:\ w_1, w_2, \Pi_{11}, \Pi_{12}, \Pi_{71}, \Pi_{72}, \Gamma_{11}$	$\dot{\Pi}_{72}:\ w_1, w_2, \Pi_{11}, \Pi_{12}, \Pi_{71}, \Pi_{72}, \Gamma_{12}$
$\dot{\Pi}_{81} = \Pi_{82} + 1$	$\dot{\Pi}_{82} = -\Pi_{81}$
$\dot{\Pi}_{91} = \Pi_{92}$	$\dot{\Pi}_{92} = 1 - \Pi_{91}$

Tab. 2: $\dot{\Pi}_{ij}$ equations.

and Π_{12}, enabling us to solve for Π_{11} and Π_{12}; deriving the latter provides explicit expressions for $\dot{\Pi}_{11}$ and $\dot{\Pi}_{12}$, from which mappings Γ_{11} and Γ_{12} can be solved. At this point, since $\dot{\Pi}_{71}$ and $\dot{\Pi}_{72}$ depend on Π_{71}, Π_{72}, and known terms, they can be dynamically implemented and are thus left as they are.

From equations $\dot{\Pi}_{61} = 0$ and $\dot{\Pi}_{62} = 0$, the values of Π_{41} and Π_{42} can be solved; finally, from the time derivatives of the latter, the remaining mappings Γ_{21} and Γ_{22} can be explicitly found. Except for the constant terms, most of the expressions above are very long; therefore, they are omitted for brevity. Nevertheless, for illustration purposes the following explicit expressions are given: $\Pi_{41} = -5(10\Pi_{71} - 1)(\Delta_1 - 9)/\Delta_2$, $\Pi_{42} = -(50\Pi_{72} - 1)(\Delta_1 - 9)/\Delta_2$, with

$$\Delta_1 = \sqrt{400\Pi_{71}w_1 - 8w_2 - 40w_1 + 400\Pi_{72}w_2 + 81},$$
$$\Delta_2 = 10w_1 + 2w_2 - 100\Pi_{71}w_1 - 100\Pi_{72}w_2.$$

Controller and observer gains: Based on the linearization $\mathbf{A} = \partial\mathbf{f}/\partial\mathbf{x}|_{\mathbf{x}=\mathbf{0}}$, $\mathbf{B} = \mathbf{g}(\mathbf{0})$, and $\mathbf{C}$, controller and observer gains $\mathbf{K}$ and $\mathbf{G}$ maximizing decay rate α_c were found via LMIs in Theorem 2.1 (referred also in Theorem 3.1) with $\mathbf{F}$ and $\mathbf{H}$ as defined therein and $\mu = 2.5\sqrt{2}$ given from TRMS parameters:

$$\mathbf{K} = \begin{bmatrix} -6.3995 & -1.0306 & -19.892 & -0.0351 & -0.0709 & -0.0029 & 75 & -21.499 & -0.0377 \\ 2.7251 & 1.3715 & 8.8202 & -1.9858 & -6.6418 & -2.1542 & -10.144 & 10.177 & -2.722 \end{bmatrix},$$

$$\mathbf{G} = \begin{bmatrix} 20.622 & -24.383 \\ -67.186 & 42.997 \\ 49.178 & 56.141 \\ 30.15 & -33.375 \\ -79.934 & 113.93 \\ 39.732 & 40.671 \\ -0.38746 & -7.1283 \\ -3.0266 & -17.494 \\ -86.575 & 46.506 \\ -86.575 & 45.506 \\ -76.285 & 96.742 \end{bmatrix}, \quad \alpha_c = 0.7.$$

Initialization: In order to generate a sinusoidal, the exosystem is initialized as $\mathbf{w}(0) = \begin{bmatrix} 0.2 & 0 \end{bmatrix}^T$; the observer as $\boldsymbol{\xi}_f(\mathbf{0}) = \mathbf{0} \in \mathbb{R}^9$ and $\boldsymbol{\xi}_s(\mathbf{0}) = \begin{bmatrix} 0.2 & 0 \end{bmatrix}^T$. Note that the exosystem is artificially constructed to generate the references; different initial conditions lead to different references which do not require any further adaptation of the nonlinear mappings $\boldsymbol{\Pi}(\cdot)$ and $\boldsymbol{\Gamma}(\cdot)$, which depend on $\mathbf{w}(t)$. As for the observer, initialization of $\boldsymbol{\xi}_f(\mathbf{0})$ can be anywhere; for simplicity, it has been assumed at "rest"; $\boldsymbol{\xi}_s(\mathbf{0})$ can also be initialized at any place, but since the current configuration allows to know where the exosystem has been initialized, it is only logical to use this knowledge in real-time. As for those mappings which are going to be dynamic, this is to say, Π_{71} and Π_{72}, initial conditions can be set anywhere since dynamic implementation enforces them to hold the FIB equations (16) – (17). Some suggestions concerning the initialization of the dynamic mappings can be found in [24], but since they require some assumptions on the plant states and the exosystem, they have not been followed in this report.

Results: Regulation results for the elevation (x_2) and the azimuth (x_5) angles are shown in Figures 3 and 4, respectively; left-hand side corresponds to simulation, right-hand side to real-time results. The corresponding control signals for elevation and az-

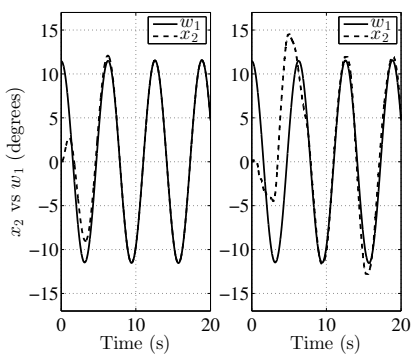

Fig. 3: Dynamic nonlinear output regulation of the elevation angle x_2: simulation (left), real-time (right).

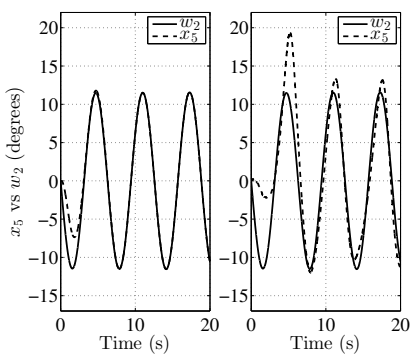

Fig. 4: Dynamic nonlinear output regulation of the azimuth angle x_5: simulation (left), real-time (right).

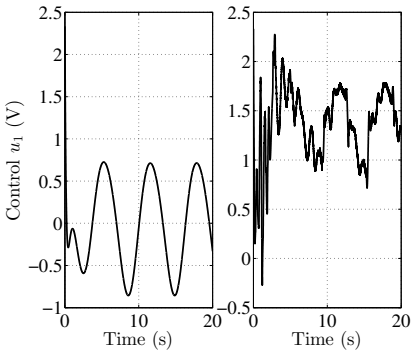

Fig. 5: Dynamic nonlinear output regulation (elevation control signal u_1): simulation (left), real-time (right).

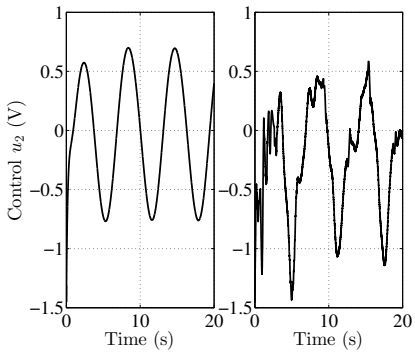

Fig. 6: Dynamic nonlinear output regulation (azimuth control signal u_2): simulation (left), real-time (right).

imuth angles, both in simulation (left) and real-time (right) are shown in Figures 5 and 6. Note that, in contrast with the simulation case, the physical setup of the twin rotor obliges the real-time control signal $u_1(t)$ to have a cd-component, this is to say, to be biased w.r.t. zero (otherwise, the beam will fall due to the counterbalance pole at its middle). Real-time implementations take advantage of any available signal: x_2 and x_5 given by the encoders, w_1 and w_2 as reference signals.

The results so far presented correspond to error-based output regulation. As a way of comparison, Figures 7 and 8, corresponding to a *state-feedback output regulation* of angles x_2 and x_5, respectively, are provided. States which are not directly measurable are read from the provider's estimators, such as x_3 (elevation angle speed) and x_6 (azimuth angle speed); others like x_8 and x_9 are obtained by integration of x_2 and x_5, respectively. Again, simulation results are shown on the left-hand side; real-time on the right one.

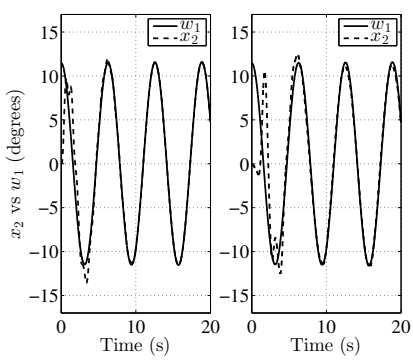

Fig. 7: Dynamic nonlinear regulation of the elevation x_2 (state feedback): simulation (left), real-time (right).

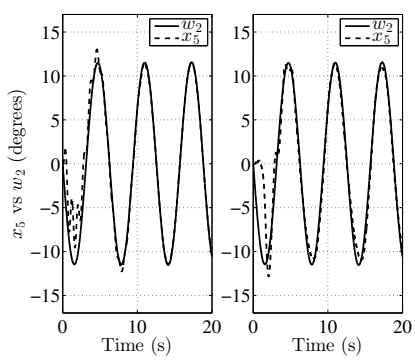

Fig. 8: Dynamic nonlinear regulation of the azimuth x_5 (state feedback): simulation (left), real-time (right).

5. CONCLUSION

An application-oriented methodology for the nonlinear error-feedback output regulation problem has been presented. It takes advantage of linear matrix inequalities for determining controller and observer gains that meet real-time requirements for the reaching phase while dynamically calculating the mappings of the steady-state phase whose explicit expressions might be too involved or impossible to find. Simulation as well as real-time implementations in a 9th-order nonlinear twin rotor, have been presented; regulation is well performed. Issues concerning the implementation as well as the solutions adopted have been discussed.

ACKNOWLEDGEMENT

This research has been supported by the ITSON PROFAPI Project CA-2016-17 as well as the ECOS Nord SEP-CONACYT ANUIES Project (France M17M08 / Mexico 291309).

(Received May 17, 2018)

REFERENCES

[1] Q. Ahmed, A. I. Bhatti, and S. Iqbal: Robust decoupling control design for twin rotor system using Hadamard weights. In: Control Applications, (CCA) and Intelligent Control, (ISIC), 2009 IEEE, pp. 1009–1014. DOI:10.1109/cca.2009.5281000

[2] M. Bernal, R. Marquez, V. Estrada, and B. Castillo: An element-wise linear matrix inequality approach for output regulation problems. In: World Automation Congress (WAC) 2012, Puerto Vallarta 2012, pp. 1–6.

[3] M. Bernal, R. Marquez, V. Estrada-Manzo, and B. Castillo-Toledo: Nonlinear output regulation via Takagi–Sugeno fuzzy mappings: A full-information LMI approach. In: IEEE International Conference on Fuzzy Systems 2012, pp. 1–7. DOI:10.1109/fuzz-ieee.2012.6251202

[4] S. Boyd, L. E. Ghaoui, E. Feron, and V. Belakrishnan: Linear Matrix Inequalities in System and Control Theory. SIAM, Studies In Applied Mathematics *15*, Philadelphia 1994. DOI:10.1137/1.9781611970777

[5] C. I. Byrnes and A. Isidori: Limit sets, zero dynamics, and internal models in the problem of nonlinear output regulation. IEEE Trans. Automat. Control *48* (2003), 10, 1712–1723. DOI:10.1109/tac.2003.817926

[6] C. I. Byrnes and A. Isidori: Nonlinear internal models for output regulation. IEEE Trans. Automat. Control *49* (2004), 12, 2244–2247. DOI:10.1109/tac.2004.838492

[7] C. I. Byrnes, F. D. Priscoli, and A. Isidori: Output regulation of uncertain nonlinear systems. Springer Science and Business Media, 2012. DOI:10.1007/978-1-4612-2020-6

[8] E. Davison: The robust control of a servomechanism problem for linear time-invariant multivariable systems. IEEE Trans. Automat. Control *21* (1976), 1, 25–34. DOI:10.1109/tac.1976.1101137

[9] G. R. Duan and H. H. Yu: LMIs in Control Systems: Analysis, Design and Applications. CRC Press, 2013.

[10] Feedback instruments Ltd, East Sussex. TRMS 33-949S User Manual: Twin Rotor MIMO System Control Experiments, 1998.

[11] B. A. Francis: The linear multivariable regulator problem. SIAM J. Control Optim. *15* (1077), 486–505. DOI:10.1137/0315033

[12] B. A. Francis and W. M. Wonham: The internal model principle for linear multivariable regulators. J. Appl. Math. Optim. *2* (1975), 170–194. DOI:10.1007/bf01447855

[13] M. Glauser, Z. Lin, and P. E. Allaire: Modeling and control of a partial body weight support system: an output regulation approach. IEEE Trans. Control Systems Technol. *18* (2010), 2, 480–490. DOI:10.1109/tcst.2009.2016953

[14] J. Henriques, P. Gil, A. Cardoso, P. Carvalho, and A. Dourado: Adaptive neural output regulation control of a solar power plant. Control Engrg. Practice *18* (2010), 10, 1183–1196. DOI:10.1016/j.conengprac.2010.06.001

[15] A. Isidori: Nonlinear Control Systems. Third edition. Springer, London 1995. DOI:10.1007/978-1-84628-615-5

[16] A. Isidori and C. I. Byrnes: Output regulation of nonlinear systems. IEEE Trans. Automat. Control *35* (1990) 2, 131–140. DOI:10.1109/9.45168

[17] T. N. Jensen, R. Wisniewski, C. DePersis, and C. S. Kallesøe: Output regulation of large-scale hydraulic networks with minimal steady state power consumption. Control Engrg. Practice *22* (2014), 103–113. DOI:10.1016/j.conengprac.2013.10.004

[18] H. Khalil: Nonlinear Systems. Third edition. Prentice Hall, New Jersey 2002.

[19] W. Kim, H. Kim, C. C. Chung, and M. Tomizuka: Adaptive output regulation for the rejection of a periodic disturbance with an unknown frequency. IEEE Trans. Control Systems Technol. *19* (2011), 5, 1296–1304. DOI:10.1109/tcst.2010.2066276

[20] F. L. Lewis, D. M. Dawson, and C. T. Abdallah: Robot Manipulator Control: Theory and Practice. CRC Press, 2003. DOI:10.1201/9780203026953

[21] R. Mahony, I. Mareels, G. Bastin, and G. Campion: Static-state feedback laws for output regulation of non-linear systems. Control Engingrg. Practice *4* (1966), 7, 1009–1014. DOI:10.1016/0967-0661(96)00100-1

[22] L. Marconi and L. Praly: Uniform practical nonlinear output regulation. IEEE Trans. Automat. Control *53* (2008), 5, 1184–1202. DOI:10.1109/tac.2008.923674

[23] J. A. Meda and B. Castillo: Synchronization of chaotic systems from a fuzzy regulation approach. Fuzzy Sets Systems *160* (2009), 19, 2860–2875. DOI:10.1016/j.fss.2008.12.006

[24] J. A. Meda, J. C. Gomez, and B. Castillo: Exact output regulation for nonlinear systems described by Takagi–Sugeno fuzzy models. IEEE Trans. Fuzzy Systems *20* (2012), 2, 235–247.

[25] F. Nejjari, D. Rotondo, V. Puig, and M. Innocenti: LPV modelling and control of a Twin Rotor MIMO system. In: 19th Mediterranean Conference on Control and Automation (MED), IEEE 2011, pp. 1082–1087. DOI:10.1109/med.2011.5983178

[26] S. K. Pandey and V. Laxmi: Optimal control of twin rotor MIMO system using LQR technique. Comput. Intell. Data Mining *31* (2015), 11–21. DOI:10.1007/978-81-322-2205-7_2

[27] A. Pavlov, B. Janssen, N. Van de Wouw, and H. Nijmeijer: Experimental Output Regulation for a Nonlinear Benchmark System. IEEE Trans. Control Systems Technol. *15* (2007), 4, 786–793. DOI:10.1109/tcst.2006.890294

[28] B. Pratap and S. Purwar: Neural network observer for twin rotor mimo system: an lmi based approach. In: The 2010 International Conference on Modelling, Identification and Control (ICMIC), IEEE 2010, pp. 539–544.

[29] R. Robles and M. Bernal: Comments on Exact output regulation for nonlinear systems described by Takagi–Sugeno fuzzy models. IEEE Trans. Fuzzy Systems *23* (2015), 1, 230–233. DOI:10.1109/tfuzz.2014.2321773

[30] K. Tanaka and H. O. Wang: Fuzzy Control Systems Design and Analysis: A Linear Matrix Inequality Approach. John Wiley and Sons, New York 2001. DOI:10.1002/0471224596

[31] C.-W. Tao, J.-S. Taur, Y.-H. Chang, and C.-W. Chang: A novel fuzzy-sliding and fuzzy-integral-sliding controller for the twin-rotor multi-input–multi-output system. IEEE Trans. Fuzzy Systems *18* (2010), 5, 893–905. DOI:10.1109/tfuzz.2010.2051447

[32] A. Tapia, R. Márquez, M. Bernal, and J. Cortez: Sliding subspace design based on linear matrix inequalities. Kybernetika *50* (2014), 3, 633–641.

[33] T. J. Tarn, P. Sanposh, D. Cheng, and M. Zhang: Output Regulation for Nonlinear Systems: Some Recent Theoretical and Experimental Results. IEEE Trans. Control Systems Technol. *13* (2005), 605–610. DOI:10.1109/tcst.2004.841674

[34] Y. Umemura and N. Sakamoto: Optimal servo design for lock-up slip control for torque converter nonlinear output regulation approach. IEEE Trans. Control Systems Technol. *23* (2015), 4, 1587–1593. DOI:10.1109/tcst.2014.2366077

[35] S. Y. Yoon, L. Di, and Z. Lin: Unbalance compensation for AMB systems with input delay: An output regulation approach. Control Engrg. Practice *46* (2016), 166–175. DOI:10.1016/j.conengprac.2015.11.002

Carlos Armenta, Sonora Institute of Technology, 5 de febrero 818 Sur, Ciudad Obregón, Sonora 85000. Mexico.
e-mail: carlos_armenta11@hotmail.com

Jorge Álvarez, Sonora Institute of Technology, 5 de febrero 818 Sur, Ciudad Obregón, Sonora 85000. Mexico.
e-mail: jorge_kookee_04@hotmail.com

Raymundo Márquez, Sonora Institute of Technology, 5 de febrero 818 Sur, Ciudad Obregón, Sonora 85000. Mexico.
e-mail: raymundo.marquez@itson.edu.mx

Miguel Bernal, Sonora Institute of Technology, 5 de febrero 818 Sur, Ciudad Obregón, Sonora 85000. Mexico.
e-mail: miguel.bernal@itson.edu.mx